Energy 190 (2020) 116385

Contents lists available at ScienceDirect

Energy

journal homepage: www.elsevier.com/locate/energy

The role of activated carbon size in the catalytic cracking of naphthalene

F. Parrillo [a], G. Ruoppolo [b], U. Arena [a, *]

[a] Department of Environmental, Biological and Pharmaceutical Sciences and Technologies, University of Campania "Luigi Vanvitelli", Via A. Vivaldi 43, 81100, Caserta, Italy
[b] Combustion Research Institute, National Research Council-CNR, P.le Tecchio 80, 80125, Naples, Italy

ARTICLE INFO

Article history:
Received 13 July 2019
Received in revised form
11 October 2019
Accepted 16 October 2019
Available online 22 October 2019

Keywords:
Tar cracking
Activated carbon
Syngas cleaning
Gasification
Biomass-to-Energy
Waste-to-Energy

ABSTRACT

Activated carbons are efficient catalysts for tar cracking, suitable for hot cleaning of the syngas produced during biomass- and waste-to-energy gasification processes. This study investigates the conversion of naphthalene, utilised as reference for tar compounds, when catalysed by a coal-derived activated carbon. The attention focuses on the influence of the operating temperature, in the range 750–900 °C, and the size of selected activated carbon, which has been used under form of pellets, granules and powders. The conversion efficiency improves when the temperature raised from 750 °C to 900 °C (from 79% to 99%, for the pellets), and when the catalyst size reduced from pellets to powders (from 79% to 97%, at 750 °C). The diffusional resistance in the catalyst particles has been then quantified in terms of Thiele modulus and internal effectiveness factor. A gradual reduction of catalyst surface area has been also observed for longer tests, due to the progressive deposition of soot from naphthalene decomposition over and inside the porous structure of the activated carbon. The carbon content of these deposits has been quantified, showing larger percentages on the surface of granules and powders.

1. Introduction

The gasification of a solid fuel (such as biomass, waste or coal) produces a syngas consisting of some major compounds (CO, H_2, CH_4, CO_2, H_2O, and N_2 when air is used as gasifying agent) and, to a lesser extent, different inorganic and organic contaminants. This fuel gas can be burned to produce electricity or further processed to produce chemicals or second-generation fuels [1]. However, it contains a not negligible amount of tar compounds, a mixture of heavy hydrocarbons condensing at temperatures below 400 °C, which strongly limits the number of its possible final applications. Different approaches have been proposed in order to reduce tar concentration [2,3]. The use of water or oil scrubbers for the physical removal of tar can reduce the tar dew point below the temperature necessary for its use in internal combustion engines for power production [4]. However, if water is used in the scrubber, this solution can appear just like a shifting of burdens, with economic and environmental implications, since the chemical energy contained in the tar is lost and the tar-contaminated liquid stream must be treated. When oil is utilised in the scrubber, the convenience of the system is greatly related to the absence of oil mist in the cleaned syngas and to the possibility to utilize the "tar containing" oil as a fuel. Some advanced concepts, such as that of Olga technology, have reached the commercial stage [5] but their complexity and costs are too high to be suitable for small and medium scale gasifiers [6]. The use of different kind of catalysts for tar conversion appears an interesting alternative. The metallic-based catalysts (such as those based on Ni, Rh, Pt, Ru) tend to deactivate rapidly due to the presence of inorganic contaminants in the raw syngas, such as hydrogen sulphide [7–9]. Several studies highlighted the use of cheap and poisoning-resistant catalysts, such as olivine and some activated carbons, as promising options for tar removal from hot syngas [10–14].

It has been found that the catalytic activity of activated carbon increases significantly at temperatures above 800 °C, allowing tar conversions on its surface close to that obtained by using expensive Ni-based catalysts [10,12]. It has been also showed that a bed of activated carbon deactivates when it is exposed to a tar-loaded gas [11,15,16], as a consequence of the coking over the surface. Increasing the temperature and/or the steam or carbon dioxide concentration above a certain level contributes to reduce or avoid

* Corresponding author.
E-mail address: umberto.arena@unicampania.it (U. Arena).

https://doi.org/10.1016/j.energy.2019.116385

Nomenclature

AK	Activated carbon
C_A	Naphthalene concentration in the gas, mg/dm^3
C_{AS}	Naphthalene concentration at the catalyst surface, mg/dm^3
D_{eff}	Effective diffusivity, m^2/s
D_K	Knudsen diffusivity, m^2/s
$D_{K,\ eff}$	Effective Knudsen diffusivity, m^2/s
D_M	Naphthalene molecular diffusivity, m^2/s
$D_{M,\ eff}$	Effective naphthalene molecular diffusivity, m^2/s
d_{pore}	Pore diameter, nm
k_c	Mass transfer coefficient, m/s
k_n	Rate coefficient of a reaction of order, n s^{-1}
k_1	Rate coefficient of a reaction of order 1, s^{-1}
L	Particle size for cylinders and spheres according to Levenspiel (1999), nm
M_i	Molecular weight, kg/kmol
m_{inlet}	Mass of naphthalene fed to the reactor, mg
m_{outlet}	Mass of naphthalene at the reactor outlet, mg
R	Ideal gas constant, J/mol K
r'_A	Measured rate of reaction, kmol/kg$_{AK}$s
R_{AK}	Radius of catalyst particle, nm
T	Temperature, °C, K

Greek symbols

H	Internal effectiveness factor, -
η_{C10H8}	Naphthalene conversion, %
ε	Bed voidage, -
θ	Char particle internal porosity, -
ρ_b	Bulk density of catalyst bed, kg/m^3
T	Tortuosity factor, -
Φ	Total pore volume, cm^3/g
Φ_n	Thiele modulus of a reaction of order n, -
Φ_1	Thiele modulus of a reaction of order 1, -

soot formation/deposition. If the rate of soot conversion by steam gasification is higher than its deposition, the activated carbon activity can be maintained over the time [11,16,17]. Moreover, it has been highlighted that steam or CO_2 activation can affect the char structure, so further influencing the reforming of tar [12,18,19]. Some recent studies report that tar conversion depends on the extension and nature of the surface available for tar cracking reaction [15,20–22]. The high activity has been related for a larger extent to the presence over the surface of oxygenated groups and alkali and alkaline earth metallic (AAEM) species [15,19,20,23–27].

An activated carbon, or activated char, is defined as "a char, which has been subjected to reaction with gases at high temperature, sometimes adding chemicals during or after carbonization in order to increase its porosity" [28]. Therefore, its physical-chemical properties mainly depend on the composition of the parent material, type of activating agent and temperature of activation process [29]. Steam activation produces chars with higher mesopore volume, while carbon dioxide activation produces higher micropore volume [17,29–31]. The concentration of catalytic elements (mainly, K and Ca) on the activated carbon surface is also enhanced by steam [12,18,19]. However, during tar conversion the original characteristics of the char changes, together with its activity [11,23]. This is due to the evolution of the pore size distribution and concentration of active groups on the surface, which also affect the balance between the rate of carbon conversion and that of soot deposition. All activated carbons contain micropores (having an internal diameter below 2 nm), mesopores (internal diameter between 2 nm and 50 nm), and macropores within their structures but the relative proportions vary considerably according to the raw material and activation process. A tar molecule has to move from the bulk gas to the catalyst external surface, and then diffuse into the pores and react over the internal surface. The role of diffusion resistance and pore mouth blocking of micropores during the conversion of naphthalene has been recently highlighted by Nestler et al. [32]. A deeper understanding of the conversion process over activated carbons could help in the selection of the best experimental conditions to minimize their deactivation and proper pretreatments to improve their physicochemical characteristics.

To this end, this study investigated the catalytic conversion of naphthalene, used as tar model compound, over a coal-derived activated carbon. The main innovative aspect of the study is that, for the first time at authors' knowledge, the possible effect of the catalyst size on the naphthalene cracking has been investigated in depth at different operating temperatures by using pellets, granules and powders of the same activated carbon, all available on the market and usually adopted in practical applications. This allows to isolate the role of activated carbon size by those of other parameters, such as the textural properties and porosity of the catalyst and the concentration of inorganic elements over its external surface.

2. Materials and methods

2.1. Sample preparation and tar model compound

A market-available Chinese coal-derived activated carbon, commercialised as NORIT RB4W, was selected among those available on the market for utilisation at temperatures above 700 °C. It is produced by pyrolysis of a Chinese coal and a further steam activation, and it is provided on the market as cylindrical pellets with 3 mm of diameter and lengths between 5 and 7 mm. These pellets have been crushed and sieved in order to obtain two different size ranges (0.8–1.2 mm and 0.3–0.4 mm) with the aim of investigating the effect of catalyst size on the tar conversion. Tar is a complex mixture of heavy hydrocarbons, and it is represented here by naphthalene. This assumption is widely used in similar research studies [33] since naphthalene represents the main and most stable component of tar mixtures obtained by gasification processes, whatever the applied technology and the feedstock utilised [34,35]. The utilisation of a nitrogen stream as carrier gas was determined by the necessity of isolating a specific effect (that of the catalyst size) and avoiding any possible misleading side effects related to other components of the syngas, such as for instance, steam, carbon dioxide or dust.

2.2. Characterization of the tested activated carbons

The ultimate analyses of the activated carbon (AK) samples were carried out by means of an elemental analyser CHN 2000 LECO, according with the ASTM D5373 procedure. The ICP-MS analyses of the samples were performed by means of an Agilent 7500CE instrument, according to US-EPA 3051 and 3052 methods. This instrument allows measurements with an error lower than 10%.

Table 1 reports the ultimate analysis of the AK, also including the amounts of some specific inorganic elements (obtained as the product of their mass fraction in the ash and the ash content of the selected activated carbon) whose catalytic activity has been often

Table 1
Ultimate and inorganic fraction analyses of the selected activated carbon.

Ultimate Analysis ($\%_{db}$)	
Carbon	78.61 ± 0.08
Hydrogen	0.69 ± 0.03
Nitrogen	0.37 ± 0.004
Oxygen (by diff.)	11.29
Ash	9.03 ± 0.12
Inorganic fraction analysis (mg/kg_{db})	
Na	57.2
K	58.2
Mg	89.2
Ca	330.8
Al	400.3
Fe	296.7
Si	625.5
Cu	0.8

recognized [13,15,19,20,26].

The materials tested have been further characterized by a series of porosimetric analyses. All the samples of the AK carbon have been preliminary kept in a nitrogen atmosphere at 750 °C for 5 min. This pre-treatment simulates the thermal history of the activated carbons in the experiments described in the following, allowing a more reliable analysis of their true characteristics at the beginning of the tests. Nitrogen adsorption/desorption were performed by a Quantachrome Autosorb 1-C analyser at 77 K, which is able to guarantees values with a deviation standard lower than 1%. Adsorption/desorption data were processed to evaluate the surface area according to BET method, and the pore size distribution according to Density Functional Theory (DFT) and Montecarlo simulation method (DFT Kernel: N_2 at 77 K on carbon, slit pore, the Non-Local Density Functional Theory (NLDFT) equilibrium model). These methods are extensively utilised for characterization of micro and mesoporous carbons [36]. The measurements have been performed on all the catalyst samples of different sizes, reported as AK pellets, AK granules and AK powder, respectively (Fig. 1).

Table 2
Porosimetric analysis and densities of AK pellets, granules and powder, after heating up to 750 °C in a nitrogen atmosphere.

	AK pellets	AK granules	AK powders
Particle size (mm)	4 × 6	0.8–1.2	0.3–0.4
Porosimetric Analysis (m^2/g)			
Specific Surface Area	904	995	993
Micropore Area	747	663	663
Mesopore Area	157	332	330
Total pore volume (cm^3/g)	0.43	0.50	0.52
Mean pore diameter (nm)	0.63	0.66	0.60
Bulk density (kg/m^3)	464	478	489
Bed Voidage, ε	0.734	0.726	0.720

The obtained adsorption isotherms are all of Type I (b), based on IUPAC Technical Report [37], which corresponds to materials having pore size distributions including micropores larger than 1 nm and also some narrow mesopores (<2.5 nm). The hysteresis loops appear limited, suggesting a microporous nature of the used catalysts. Table 2 reports the porosimetric analyses for the activated carbon under form of pellets, granules, and powders, which all support this conclusion. According with these data, the crushing process necessary to prepare AK granules and powders from the pellets does not significantly influence the internal structure of the chars. The market available activated carbon, under its various forms of pellets, granules and powder, always shows a high specific surface area.

2.3. Experimental apparatus

Naphthalene conversion tests have been carried out in the experimental apparatus sketched in Fig. 2, which shows its main sections: feeding system, reactor, sampling/cleaning device and gas analyser.

The feeding system consists of a rotameter for adjusting the nitrogen flowrate and a naphthalene saturator to obtain the tar-

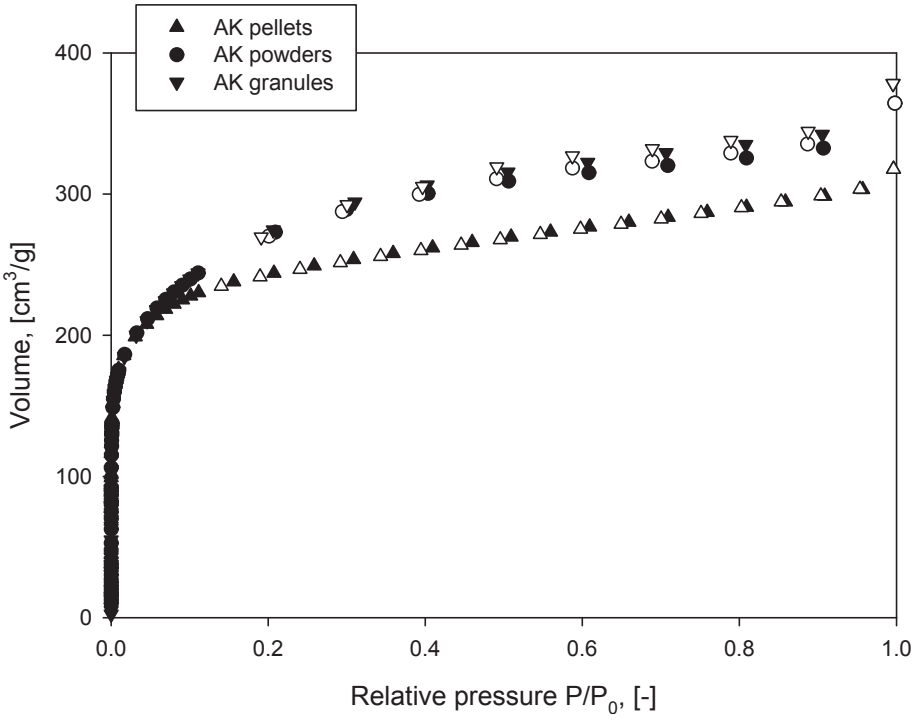

Fig. 1. Isotherm curves of nitrogen adsorption (shaded symbols) and desorption (open symbols) at 77 K.

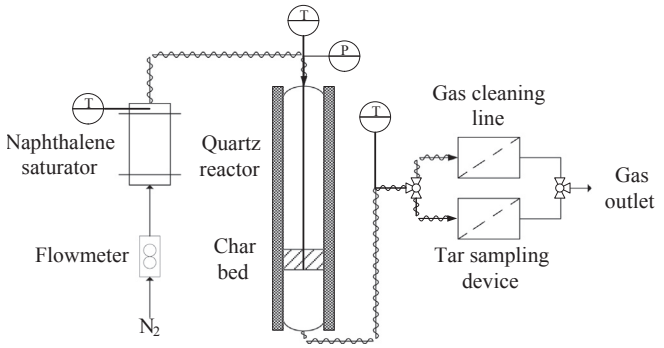

Fig. 2. Sketch of the experimental apparatus used for the naphthalene conversion tests.

doped stream. The pipes between the saturator and the reactor were kept above 150 °C to avoid naphthalene condensation. The reactor used is a vertical tubular quartz reactor with an internal diameter of 14 mm and a total height of 600 mm. The bed of activated carbons was placed above a glass frit inside the reactor, located at 430 mm from the top. The bed temperature was measured in the centre of the bed by means of a K type thermocouple. The gas at the exit of the reactor was directed to the sampling device during the tar samplings and to the cleaning device for the rest of the time, by switching a three-ways valve. The sampling device consists of three impingers, filled with isopropanol at 0 °C. Dedicated experiments showed a capture efficiency of this device above 99%, under the conditions analysed in this study. The gas at the exit of the cleaning section was analysed by means of a micro-GC with a thermal conductivity detector (TCD) for the online determination of short chain hydrocarbons (from acetylene to benzene) and molecular hydrogen. Further details on the experimental apparatus can be found elsewhere [13].

2.4. Experimental conditions and procedure

Table 3 reports the experimental conditions of all the tests. Each test has been repeated three times and carried out with an activated carbon bed height of 3 cm and an effective gas residence time of 0.11 s. The latter has been calculated by dividing the bed height to the effective gas velocity (i.e. the superficial gas velocity divided by the bed voidage reported in Table 2) at the operating temperature. There is a very limited difference between these residence times (0.107 s–0.110 s, depending on the size of the AK and the nitrogen flowrate) that does not affect the obtained conversion efficiencies.

The first set of experiences (set #1) investigated the initial conversion of naphthalene. The reactor, with the char bed inside, was heated at the desired temperature in an atmosphere of pure nitrogen. The investigated temperature range of 750–900 °C has been defined by taking into account the syngas temperature at the exit of fluidized bed gasifiers operated at different high equivalence ratios and/or with biomass or waste of different low heating value [38]. When system reached the desired temperature, the nitrogen flow was sent to the naphthalene saturator to obtain a gas stream with a naphthalene concentration of 22.5 mg/NL. After 5 min of reaction and gas composition stabilization, the gas was sampled for 2 min. The reactor was then purged, and cooled down with pure nitrogen. The effect of the temperature on the thermal decomposition of naphthalene was evaluated by using inert particles (silica sand) instead of activated carbons in the reactor. The reactor temperature was increased from 400 °C to 900 °C with the aim of evaluating the impact of the bed temperature on the tar conversion. As expected [32,39,40], the thermal conversion of naphthalene resulted negligible under all the conditions tested, highlighting its high thermal stability, even at the highest temperature. A series of preliminary tests also showed that the selected AK has a cracking efficiency higher than those of natural and synthetic catalysts of the same size sometime used in hot syngas cleaning devices, such as olivine, alumina, calcined dolomite [2,10,33,41]. In particular, at 750 °C the powders of the selected AK provide a naphthalene conversion efficiency of 97.1%, i.e. 23% higher than that of calcined dolomite (which has an efficiency of 73.6%), 31% than that of alumina (66.2%), and 23% than that of olivine (64.1%), respectively.

The second kind of experiences (set #2) investigated the evolution with time of the naphthalene conversion for the different catalysts tested. The test durations ranged from 5 to 213 min while the temperature was maintained at 750 °C. Gas samples were taken during the tests to measure the naphthalene concentration in the exit gas at different times.

Table 3
Experimental conditions tested.

Experimental set	# 1			# 2
Activated carbon	Pellets, Granules and Powders			
Nitrogen flowrate, NL/min	0.49	0.47	0.43	0.49
Temperature, °C	750	800	900	750
Total time test, min	7	7	7	>200

2.5. Data analysis

The determination of the naphthalene concentration in the isopropanol samples was performed by means of a gas chromatograph coupled with mass spectrometer (GC-MS Agilent HP6890/HP5975, equipped with a capillary column DB-5MS, 60 m × 0.25 mm ID). The naphthalene conversion was estimated as:

$$\eta_{C10H8} = \frac{m_{inlet} - m_{outlet}}{m_{inlet}} \quad (1)$$

where m_{inlet} is the mass of naphthalene fed to the reactor and m_{outlet} is the mass of naphthalene recovered in the impinger bottles at different sampling times. A tar molecule (that here is assumed to be a naphthalene molecule) has to move from the gas phase to the external surface of the activated carbon particle and then diffuse into the pores to be catalytically converted over the internal surface. The Thiele modulus has been then calculated to investigate the effect of catalyst particle size on the naphthalene conversion rate. It represents the ratio of the intrinsic rate of chemical reaction to the rate of diffusion through the particle [42,43]:

$$\Phi_n^2 = \frac{k_n R_{AK}^2 C_{As}^{n-1}}{D_e} \quad (2)$$

where k is the rate coefficient of the reaction of order n calculated as in a previous study [13], R_{AK} is the catalyst particle radius, C_{As} is the reactant concentration at the catalyst surface and D_e is the effective diffusivity. It can be assumed that the bulk reactant concentration, C_A (mol/dm^3), is equal to C_{As}. This assumption has been validated by the Mears' Criterion for external diffusion [43]: there is no film diffusion resistance when:

$$\frac{-r_A' \rho_b R_{AK} n}{k_c C_A} < 0.15 \quad (3)$$

where r_A' is the measured rate of reaction (kmol/kg$_{AK}$ s), ρ_b is the bulk density of catalyst bed (kg/m^3), and k_c is the mass transfer

coefficient (m/s). The obtained values range from 0.0062 for AK powders at 750 °C to 0.034 for AK pellets at 900 °C, and then it is reasonable to assume that no concentration gradients exist between the bulk gas and external surface of the catalyst material ($C_A = C_{As}$). Therefore, assuming a reaction of the first order with respect to the naphthalene concentration at high temperatures [13,15], the Thiele modulus can be simplified as:

$$\Phi_1 = L\sqrt{\frac{k_1}{D_{eff}}} \tag{4}$$

where $L = R_{AK}/2$ for cylindrical particle, such as the utilised pellets, and $L = R_{AK}/3$ for spherical particles, such as the utilised granules and powders can be assumed to be [44]. The effective diffusivity takes into account that the pores in the pellet are not straight and cylindrical but a series of a tortuous and interconnected paths with pore throats varying cross-sectional areas. Characteristic values of D_{eff} for gases and liquids in porous solids can be calculated by the following equation [45,46]:

$$\frac{1}{D_{eff}} = \frac{1}{D_{K,\,eff}} + \frac{1}{D_{M,\,eff}} \tag{5}$$

where D_K is the effective Knudsen diffusivity and D_M is the naphthalene effective molecular diffusivity [44], which has been estimated as [45,46]:

$$D_{M,\,eff} = D_M\frac{\theta}{\tau} \tag{6}$$

where D_M is the naphthalene molecular diffusivity, θ is the char particle internal porosity and τ is the tortuosity factor (assumed equal to 4 based on the study of Leyva-Ramos [47]). The effective Knudsen diffusivity has been calculated by using the following equation:

$$D_{K,\,eff} = \left(\frac{d_{pore}}{3}\sqrt{\frac{8RT}{\pi M_i}}\right)\frac{\theta}{\tau} \tag{7}$$

where d_{pore} is the average pore diameter (nm), R is the gas constant (8.314 J/mol K), T is the temperature (K), M_i the molecular weight (kg/mol).

Finally, the measure of "how much the reaction rate is lowered because of the resistance to pore diffusion" is given by the effectiveness factor. It is defined as the ratio between the "actual mean reaction rate within the pore" and the same "rate if not slowed by pore diffusion", i.e. the rate that would result if the interior surface was exposed to the external pellet surface conditions [44]. It has been then calculated as a function of the Thiele modulus, by the equation:

$$\eta = \frac{3}{\Phi_1^2}\left(\Phi_1 coth\Phi_1 - 1\right) \tag{8}$$

3. Results and discussion

The influence of particle size during naphthalene conversion over AK has been investigated by using three different sizes of the activated carbon, at temperatures between 750 °C and 900 °C, and with a gas residence time of the tar-loaded gas in the char bed of 0.11s. The histograms of Fig. 3 describe the initial conversion of naphthalene. At 750 °C and 800 °C there is a clear influence of the size of the activated carbon on the conversion of naphthalene: the finer material improves the naphthalene conversion efficiency, which increases from 79% for pellets to 97% for powders, at 750 °C, and from 81% for pellets to 100% for powders, at 800 °C.

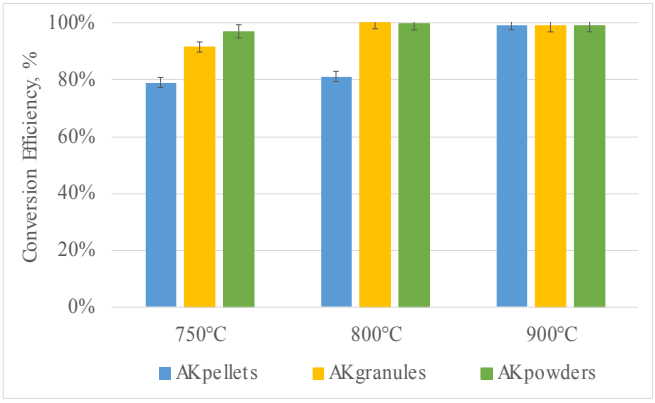

Fig. 3. Naphthalene conversion obtained with AK pellets, granules and powders at 750 °C, 800 °C, 900 °C, reported as percentage and with the indication of the standard deviation.

This result is further supported by the initial higher increase of hydrogen generation at 750 °C, which is related to the higher tar conversion (Fig. 4).

Fig. 5 reports the time evolution of the naphthalene conversion at 750 °C for the three particle sizes during the tests, showing the continuous reduction of the conversion efficiency related to the progressive decrease of available surface area. The results, reported with error bars indicating the standard deviation, suggest a rather similar behaviour of AK granules and powders while the AK pellets always show lower conversion efficiencies, for 10% or more. This indicates that smaller particles imply a reduced diffusional resistance.

The experimental activity also determined the evolution of bed material weight AK pellets, granules and powders at 750 °C (Fig. 6), by performing ultimate analyses of fresh and gradually exhausted samples. The cumulative amount of carbon deposit was slightly higher for AK granules and AK powders, suggesting an easier contact between the naphthalene molecule and the catalytic elements of the inorganic fraction, such as iron and the AAEMs. The measured increase of carbon contents in the char, also reported in Fig. 6, from about 79% to about 84%, confirms the production and deposition of soot, according to the carbonization reaction: $C_{10}H_8 \rightarrow 10\,C + 4H_2$.

This aspect can be further investigated by means of a scanning electron microscopy, by analysing images of the materials at the beginning and the end of each test, as obtained by means of a FEI Inspect™ S50 SEM (Fig. 7), and focusing the attention on the pore size [48]. Large part of the numerous pores of the fresh material (top of Fig. 7) is no longer present after the test (bottom of Fig. 7). The carbon deposits from naphthalene carbonization are largely present on the AK surface at the end of the test, under form of small grains, generally concentrated around specific areas of the surface, probably corresponding to active sites. Similar carbon grains and filament have been already observed over activated carbons from coals or coconut shells, and also in these cases their formation was related to the catalytic activity of iron and alkali species [49]. In the SEM image of the AK pellet, it is also possible to individuate a deep fracture, which could be a consequence of thermal stresses.

Observations reported above are further supported by the evolution of pore distribution in AK pellets, granules, and powders, as obtained by collecting the bed material at different times, under the experimental conditions of test at 750 °C (Table 4). As expected,

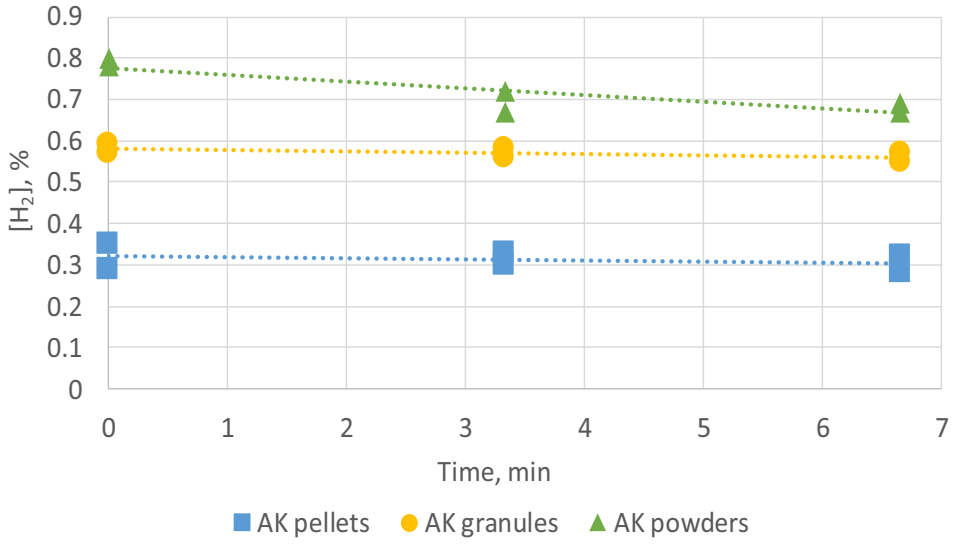

Fig. 4. Initial hydrogen generation at 750 °C for the AK pellets, AK granules and AK powders.

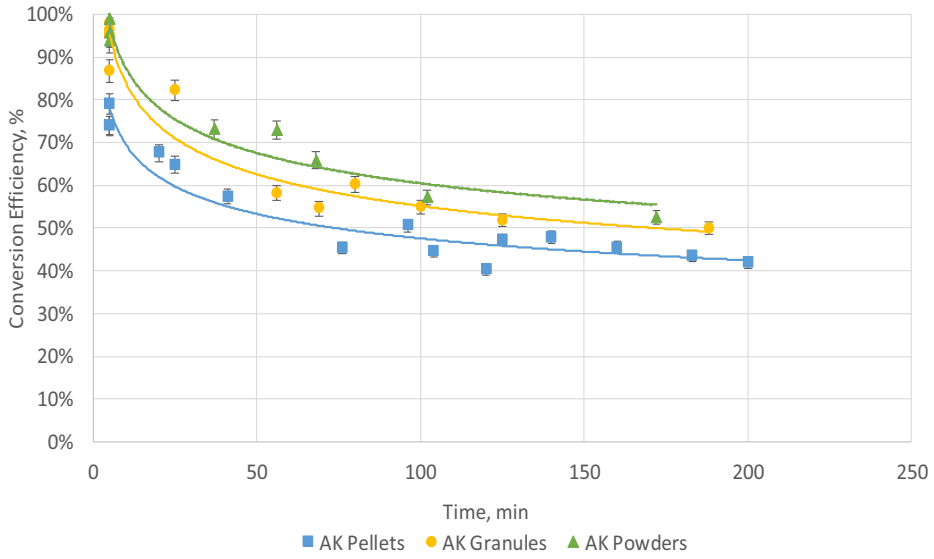

Fig. 5. Time evolution of naphthalene conversion for AK pellets, granules and powders at 750 °C.

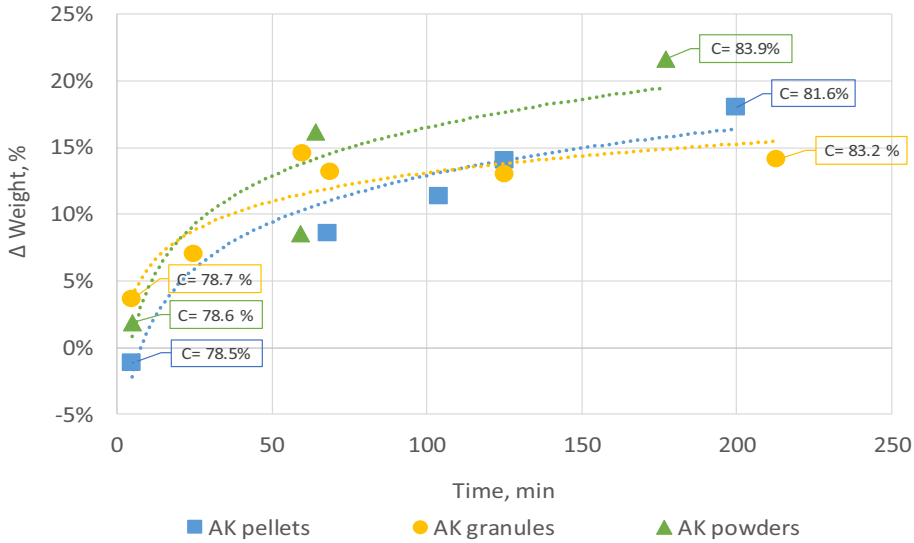

Fig. 6. Cumulative amount of deposit on the material bed for AK pellets, granules and powders at 750 °C.

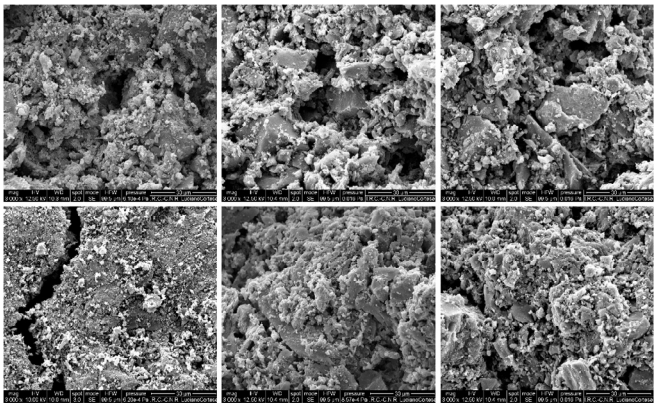

Fig. 7. SEM images of AK pellets, AK granules and AK powders, before the tests (top) and after the tests (bottom) of naphthalene conversion at 750 °C. Magnification = 3000×.

Table 4
The evolution of pore distribution for AK pellets, granules, and powders at 750 °C.

	Time, min	Specific Surface Area, m^2/g	Micropore Area, m^2/g	Mesopore Area, m^2/g
AK pellets	0	904	747	157
	72	395	273	122
	113	377	287	90
	200	75	34	41
AK granules	0	995	663	332
	63	560	378	378
	72	320	199	121
	125	233	83	150
	213	157	74	83
AK powders	0	993	663	330
	59	523	350	173
	64	430	253	177
	177	71	22	49

a progressive reduction of the total surface area and that of both mesopores and micropores, can be observed also in this case, in agreement with the progressive deposition of soot suggested by Figs. 6 and 7.

The conversion efficiencies data were finally processed to estimate the Thiele modulus and the internal effectiveness factor. The above described methodology was applied under the assumption of steady state conditions, which essentially means that the time for char deactivation is much higher than the naphthalene conversion, so that the initial conversion can be assumed as constant over time. Table 5 reports the diffusion characteristics together with the rate coefficient at three different temperatures.

As expected from the experimental results, the rate coefficient is lower for pellets at 750 °C and 800 °C, and increases with increasing temperature, reaching a maximum, which is rather comparable for AK pellets, granules and powders, at 900 °C. The effect of catalyst size appears clear by the values of the effective diffusivity, D_{eff}. These data have been then utilised to obtain the Thiele modulus and the internal effectiveness factor, reported in Table 6.

Table 5
$D_{M\ eff}$, $D_{K\ eff}$, D_e and rate coefficient for AK pellets, AK granules and AK powders at 750 °C, 800 °C and 900 °C.

T, °C	AK	$D_{M\ eff} * 10^7$, m^2/s	$D_{K\ eff} * 10^8$, m^2/s	$D_{eff} * 10^8$, m^2/s	k, s^{-1}
750	Pellets	2.16	1.63	1.51	14.08
	Granules	2.52	1.98	1.84	22.65
	Powders	2.62	2.06	1.91	32.54
800	Pellets	2.16	1.66	1.55	15.17
	Granules	2.52	2.03	1.88	42.30
	Powders	2.62	2.11	1.95	42.30
900	Pellets	2.16	1.74	1.61	46.23
	Granules	2.52	2.12	1.96	41.77
	Powders	2.62	2.21	2.03	42.31

Table 6
Thiele modulus and internal effectiveness factor for AK pellets, AK granules and AK powders at 750 °C, 800 °C and 900 °C.

T, °C	AK	φ_1	η
750	Pellets	9.17	0.292
	Granules	1.93	0.816
	Powders	0.80	0.960
800	Pellets	9.41	0.285
	Granules	2.61	0.721
	Powders	0.90	0.949
900	Pellets	16.1	0.175
	Granules	2.54	0.731
	Powders	0.88	0.951

When the particle diameter reduces from 3 mm of the AK pellets to 0.35 mm of AK powders, the Thiele modulus, φ_1, decreases from 9.17 to 0.80 at 750 °C and the effectiveness factor, η, approaches 1 (assuming the absence of a temperature gradient inside the particle). This confirms that the reaction is limited by the pore diffusion resistance for catalyst pellets. On the contrary, the small value of the Thiele modulus for AK powders suggests that the reactant is able to spread throughout the catalyst particle. This allows the powders to utilize all the available porous volume ensuring higher conversion efficiencies with respect to the AK pellets. It is also known that fine solids are free (or rather free) of diffusional effect but may create problems in their utilisation due to the potential high pressure drop. It is desirable to have the largest particle size that is still free of pore diffusion resistance, with a Thiele modulus of about 0.4 [44]. Then, the utilised catalyst powders could be rather close to the optimum size.

Finally, the results also show that the pore diffusion resistance increases with the temperature increase, but the effect is negligible for AK powders, and rather limited for AK granules. It cannot be observed in terms of conversion efficiencies because in the reported tests the complete conversion of naphthalene was already achieved at 900 °C.

4. Conclusions

The study investigated the conversion of naphthalene when it is catalysed by a coal-derived activated carbons available on the market, in a fixed bed configuration. The attention focused on the influence that the activate carbon size and the reactor temperature may have on the cracking efficiency. The internal structure of the tested activated carbons (pore size distribution and total surface area) has been measured before and after each test.

An increase in the reactor temperature and a decrease in the size of the activated carbon lead always to an increase in the naphthalene conversion. At 750 °C, its cracking efficiency increases from 79% to 97% when the particle size reduced from pellets (3 mm of diameter and lengths between 5 and 7 mm) to powders (0.3–0.4 mm). These efficiencies indicate a higher pore diffusion resistance of char pellets (with a Thiele modulus of 9.17 and an internal effectiveness factor of 0.292) while the char powders (with a Thiele modulus of 0.80 and an internal effectiveness factor of 0.960) are able to utilize all the available porous volume. In a practical application, the high pressure drop related to the utilisation of catalyst powders should be taken into account. The obtained results indicate that the analysed catalyst powders (having a

diameter in the range 0.3–0.4 mm) have a limited pore diffusion resistance without leading to high pressure drops.

The data obtained after 5-min test have been confirmed in the long tests. Anyway, when the experimental conditions were maintained up to 200 min, a further phenomenon influences the conversion mechanism. There is a gradual reduction of the surface area as a consequence of the progressive deposition of soot, coming from the catalytic cracking of naphthalene, over the porous structure of the char. The carbon content of these deposits has been quantified, showing higher percentages on the surface of granules and powders.

The practical implication of the observed gradual reduction of the surface area is that the bed of catalyst has to be periodically removed and substituted with a bed of fresh activated carbons. Future work will aim at avoiding this necessity, by investigating the mechanism (and identifying the operating conditions) by which steam or carbon dioxide may be able to continuously remove carbon deposits from the catalyst surface.

Acknowledgements

The study has been developed in the framework and with the financial support of Regione Campania, project BIOVALUE, PON/03PE_00176 (part of the activities of Smart Power System). The authors would like also to thank the “Programma VALERE 2019” of the University of Campania “Luigi Vanvitelli” that supported the experimental activities.

The contribution of Dr Diego Fuentes-Cano, of the Chemical and Environmental Engineering Department of the University of Seville, in the preliminary part of the experimental activity is greatly acknowledged. The authors also appreciate the support of Mr. Luciano Cortese, Mr. Andrea Bizzarro and Mr. Ferdinando Stanzione to SEM and porosimetry analyses.

References

[1] Arena U. Fluidized bed gasification. In: Scala F, editor. Chap. 17 in fluidized-bed technologies for near-zero emission combustion and gasification. Woodhead Publishing; 2013, ISBN 978-0-85709-541-1. p. 765–812.
[2] Li C, Suzuki K. Tar property, analysis, reforming mechanism and model for biomass gasification, an overview. Renew Sustain Energy Rev 2009;13:594–604.
[3] Xu C, Donald J, Byambajav E, Ohtsuka Y. Recent advances in catalysts for hot-gas removal of tar and NH3 from biomass gasification. Fuel 2011;89:1784–95.
[4] Phuphuakrat T, Namioka T, Yoshikawa K. Absorptive removal of biomass tar using water and oily materials. Bioresour Technol 2011;102:543–9.
[5] Emmen RMP, van der Heijden SP. Full-scale demonstration of OLGA-technology (including tar electrostatic precipitator). Final report of the projects “tar electrostatic precipitator (TEP) for OLGA-installation” and “Full-scale demonstration of the OLGA-technology”. 2010.
[6] Gómez-Barea A, Leckner B. Gasification of biomass and waste. In: Lackner M, Winter F, Agarwal AK, editors. Handbook of combustion. vol. 4. Weinheim: Wiley-VCH; 2009. p. 365–97.
[7] Hepola PS. Sulphur poisoning of nickel-based hot gas cleaning catalysts in synthetic gasification gas I. Effect of different process parameters. Appl Catal, B 1997;14:287–303.
[8] Tomishige K, Asadullah M, Kunimori K. Syngas production by biomass gasification using Rh/CeO2/SiO2 catalysts and fluidized bed reactor. Catal Today 2004;89:389–403.
[9] Ammendola P, Cammisa E, Chirone R, Lisi L, Ruoppolo G. Effect of sulphur on the performance of Rh–$LaCoO_3$ based catalyst for tar conversion to syngas. Appl Catal B Environ 2012;113–114:11–8.
[10] Abu el-Rub Z, Bramer EA, Brem G. Experimental comparison of biomass chars with other catalysts for tar reduction. Fuel 2008;87:2243–52.
[11] Di Gregorio F, Parrillo F, Cammarota F, Salzano E, Arena U. Removal of naphthalene by activated carbons from hot gas. Chem Eng J 2016;291:244–53.
[12] Feng D, Zhao Y, Zhang Y, Gao J, Sun S. Changes of biochar physiochemical structures during tar H_2O and CO_2 heterogeneous reforming with biochar. Fuel Process Technol 2017;165:72–9.
[13] Fuentes Cano D, Parrillo F, Ruoppolo G, Gomez Barea A, Arena U. The influence of the char internal structure and composition during heterogeneous naphthalene conversion. Fuel Process Technol 2018;172:125–32.
[14] Ardolino F, Lodato C, Astrup TA, Arena U. Energy recovery from plastic and biomass waste by means of fluidized bed gasification: a life cycle inventory model. Energy 2019;165:299–314.
[15] Hosokai S, Kumabe K, Ohshita M, Norinaga K, Li CZ, Hayashi JI. Mechanism of decomposition of aromatics over charcoal and necessary condition for maintaining its activity. Fuel 2008;87:2914–22.
[16] Fuentes-Cano D, Gómez-Barea A, Nilsson S, Ollero P. Decomposition kinetics of model tar compounds over chars with different internal structure to model hot tar removal in biomass gasification. Chem Eng J 2013;228:223–1233.
[17] Feng D, Zhang Y, Zhao Y, Sun S, Gao J. Improvement and maintenance of biochar catalytic activity for in-situ biomass tar reforming during pyrolysis and H_2O/CO_2 gasification. Fuel Process Technol 2018;172:106–14.
[18] Feng D, Zhao Y, Zhang Y, Sun S. Effects of H_2O and CO_2 on the homogeneous conversion and heterogeneous reforming of biomass tar over biochar. Int J Hydrogen Energy 2017;42:13070–84.
[19] Feng D, Zhao Y, Zhang Y, Zhang Z, Sun S. Roles and fates of K and Ca species on biochar structure during in-situ tar H2O reforming over nascent biochar. Int J Hydrogen Energy 2017;42:21686–2169.
[20] Feng D, Zhao Y, Zhang Y, Zhang Z, Zhang L, Gao J, Sun S. Synergetic effects of biochar structure and AAEM species on reactivity of H_2O-activated biochar from cyclone air gasification. Int J Hydrogen Energy 2017;42:16045–53.
[21] Choi C, Shima K, Kudo S, Norinaga K, Gao X, Hayashi Ji. Continuous monitoring of char surface activity toward benzene. Carbon Resour. Conver. 2019;2:43–50.
[22] Korus A, Szlęk A, Samson A. Physicochemical properties of biochars prepared from raw and acetone extracted pine wood. Fuel Process Technol 2019;185:106–16.
[23] Moliner R, Suelves I, Lazaro M, Moreno O. Thermocatalytic decomposition of methane over activated carbons: influence of textural properties and surface chemistry. Int J Hydrogen Energy 2005;30:293–300.
[24] Matsuhara T, Hosokai S, Norinaga K, Matsuoka K, Li CZ, Hayashi JI. In-situ reforming of tar from the rapid pyrolysis of a brown coal over char. Energy Fuels 2010;24:76–83.
[25] Mani S, Kastner JR, Juneja A. Catalytic decomposition of toluene using a biomass derived catalyst. Fuel Process Technol 2013;114:118–25.
[26] Feng D, Zhao Y, Zhang Y, Sun S, Meng S, Guo Y, Huang Y. Effects of K and Ca on reforming of model tar compounds with pyrolysis biochars under H_2O or CO_2. Chem Eng J 2016;306:422–32.
[27] Ravenni G, Sárossy Z, Ahrenfeldt J, Henriksen UB. Activity of chars and activated carbons for removal and decomposition of tar model compounds–A review. Renew Sustain Energy Rev 2018;94:1044–56.
[28] Köchling KH, McEnaney B, Müller S, Fitzer E. International committee for characterization and terminology of carbon. Carbon 1985;23:601–3.
[29] Guizani C, Jeguirim M, Gadiou R, Escudero Sanz FJ, Salvador S. Biomass char gasification by H_2O, CO_2 and their mixture: evolution of chemical, textural and structural properties of the chars. Energy 2016;112:133–45.
[30] Rodríguez-Reinoso F, Molina-Sabio M, González MT. The use of steam and carbon dioxide as activating agents in the preparation of activated carbons. Carbon 1995;33:15–23.
[31] Wang Y, Chen X, Yang S, He X, Chen Z, Zhang S. Effect of steam concentration on char reactivity and structure in the presence/absence of oxygen using Shengli brown coal. Fuel Process Technol 2015;135:174–9.
[32] Nestler F, Burhenne L, Amtenbrink MJ, Aicher T. Catalytic decomposition of biomass tars: the impact of wood char surface characteristics on the catalytic performance for naphthalene removal. Fuel Process Technol 2016;145:31–41.
[33] Devi L, Ptasinski KJ, Janssen FJ. Decomposition of naphthalene as a biomass tar over pretreated olivine: effect of gas composition, kinetic approach and reaction scheme. Ind Eng Chem Res 2005;44:9096–104.
[34] Arena U, Di Gregorio F, Santonastasi M. A techno-economic comparison between two design configurations for a small scale, biomass-to-energy gasification based system. Chem Eng J 2010;162:580–90.
[35] Arena U, Di Gregorio F. Gasification of a solid recovered fuel in a pilot scale fluidized bed reactor. Fuel 2014;117:528–36.
[36] Landers J, Yu G, Neimark V. Colloids and Surfaces A:P physicochemical and engineering aspects. Density functional theory methods for characterization of porous materials, vol. 437; 2013. p. 3–32.
[37] Thommes M, Kaneko K, Neimark AV, Olivier JP, Rodriguez-Reinoso F, Rouquerol J, Sing KSW. IUPAC Technical Report. Physisorption of gases, with special reference to the evaluation of surface area and pore size distribution (IUPAC Technical Report). Pure Appl Chem 2015;87(9–10):1051–69.
[38] Lopez G, Artetxe M, Amutio M, Alvarez J, Bilbao J, Olazar M. Recent advances in the gasification of waste plastics. A critical overview. Renew Sustain Energy Rev 2018;82:576–96.
[39] Bruinsma OSL, Tromp PJJ, De Sauvage Nolting HJJ, Moulijn JA. Gas phase pyrolysis of coal-related aromatic compounds in a coiled tube flow reactor 2. Heterocyclic compounds, their benzo and dibenzo derivatives. Fuel 1988;67:334–40.
[40] Jess A. Mechanisms and kinetics of thermal reactions of aromatic hydrocarbons from pyrolysis of solid fuels. Fuel 1996;75:1441–8.
[41] Rapagnà S, Virginie M, Gallucci K, Courson C, Di Marcello M, Kiennemann A, Foscolo PU. Fe/olivine catalyst for biomass steam gasification: preparation, characterization and testing at real process conditions. Catal Today 2011;176:163–8.
[42] Satterfield CN. Mass transfer in heterogeneous catalysis. 1970. p. 33–47. Cambridge.
[43] Fogler HS. Elements of chemical reaction engineering. fourth ed. Pearson

Education Inc; 2006.
[44] Levenspiel O. Chemical reaction engineering. third ed. J. Wiley&Sons Inc; 1999, ISBN 0-471-25424-X.
[45] Landi G, Barbato PS, Di Benedetto A, Pirone R, Russo G. High pressure kinetics of CH_4, CO and H_2 combustion over $LaMnO_3$ catalyst. Appl Catal B Environ 2013;134–135:110–22.
[46] Scala F, Solimene R, Montagnaro F. Fundamental of fluidized bed combustion and gasification. In: Scala F, editor. Chap. 7 in fluidized-bed technologies for near-zero emission combustion and gasification. Woodhead Publishing; 2013, ISBN 978-0-85709-541-1. p. 765–812.
[47] Leyva-Ramos R. Diffusion in liquid-filled pores of activated carbon. I. Pore volume diffusion. Can J Chem Eng 1994;72.
[48] Achaw OW. A study of the porosity of activated carbons using the scanning electron Microscope. Scanning Electron Microsc 2012. https://doi.org/10.5772/36337.
[49] Shen Y. Chars as carbonaceous adsorbents/catalysts for tar elimination during biomass pyrolysis or gasification. Renew Sustain Energy Rev 2015;43:281–95. https://doi.org/10.1016/j.rser.2014.11.061.